

# Lagrangian data in a high-resolution numerical simulation of the North Atlantic

## I. Comparison with in situ drifter data

Zulema D. Garraffo <sup>a,\*</sup>, Arthur J. Mariano <sup>a</sup>, Annalisa Griffa <sup>a,b</sup>, Carmela Veneziani <sup>a</sup>,  
Eric P. Chassignet <sup>a</sup>

<sup>a</sup> RSMAS / MPO, University of Miami, 4600 Rickenbacker Causeway, Miami, FL 33149, USA

<sup>b</sup> IOF / CNR, La Spezia, Italy

Received 1 November 1999; accepted 11 September 2000

---

### Abstract

A model/data comparison was performed between simulated drifters from a high-resolution numerical simulation of the North Atlantic and a data set from in situ surface drifters. The comparison makes use of pseudo-Eulerian statistics such as mean velocity and eddy kinetic energy, and Lagrangian statistics such as integral time scales. The space and time distribution of the two data sets differ in the sense that the in situ drifters were released inhomogeneously in space and time while the simulated drifters were homogeneously seeded at the same time over a regular 1° grid. Despite this difference, the total data distributions computed over the complete data sets show some similarities that are mostly related to the large-scale pattern of Ekman divergence/convergence.

Comparisons of eddy kinetic energy and root mean square velocity indicate that the numerical model underestimates the eddy kinetic energy in the Gulf Stream extension and in the ocean interior. In addition, the model Lagrangian time scales are longer in the interior than the in situ time scales by approximately a factor of 2. It is suggested that this is primarily due to the lack of high-frequency winds in the model forcing, which causes an underestimation of the directly forced eddy variability. Regarding the mean flow, the comparison has been performed both qualitatively and quantitatively using James' statistical test. The results indicate that over most of the domain, the differences between model and in situ estimates are not significant. However, some areas of significant differences exist, close to high-energy regions, notably around the Gulf Stream path, which in the model lies slightly north of the observed path, although its strength and structure are well represented overall. Mean currents close to the buffer zones, primarily the Azores Current, also exhibit significant differences between model results and in situ estimates. Possibilities for model improvement are discussed in terms of forcings, buffer zone implementations, turbulence and mixed layer parameterizations, in light of our model/data comparison. © 2001 Elsevier Science B.V. All rights reserved.

*Keywords:* Lagrangian data; Mean velocity; Eddy kinetic energy

---

\* Corresponding author. Tel.: +1-305-361-4882.

E-mail address: z.garraffo@miami.edu (Z.D. Garraffo).

## 1. Introduction

Numerical ocean circulation models are becoming more accurate in their simulations of ocean flow, primarily due to the increasing computational power that allows higher grid resolution and more complex dynamics. Despite this improvement, as well as the availability of more accurate data for initial conditions, boundary conditions, and forcing fields, the question of how “realistic” high-resolution numerical model simulations of oceanic flow really are is still open. A quantitative assessment of model skills requires a comparison of the model results with in situ ocean data on space/time scales comparable to those of the model. For large-scale basin models, this implies the use of observational data with extensive horizontal, vertical, and temporal coverage, so that both large- and synoptic-scale quantities can be evaluated. In this paper, we take a first step in this direction by comparing simulated surface (mixed layer) drifters from a high-resolution ( $1/12^\circ$ , 6-km average grid spacing) numerical simulation of the North Atlantic to in situ near-surface drifters. Lagrangian data have been previously used in model/data comparisons (e.g. Davis, 1996), especially using pseudo-Eulerian estimates such as the mean flow (e.g. Acero-Schertzer et al., 1997; Stutzer and Krauss, 1998). In the following sections, a quantitative comparison of the mean flow is performed together with a qualitative comparison of other statistics, both Eulerian and Lagrangian.

The ocean numerical model is the Miami Isopycnic Coordinate Ocean Model (MICOM), configured with realistic topography and stratification, a Kraus–Turner mixed layer parameterization, and forcing by monthly climatology from the Comprehensive Ocean-Atmosphere Data Set (COADS). A set of numerical drifter trajectories was computed in the uppermost layer of the model (mixed layer), and their statistics are compared with those of in situ near-surface drifter data, processed and archived at the WOCE/CLIVAR Drifter Data Assembly Center at NOAA-AOML. The in situ drifters are drogued with a 10-m holey sock centered at a depth of 15 m. Trajectories of these satellite-tracked near-surface drifters used in our study span the time period between 1989 and 1998.

The comparison is performed using two main types of statistics: (a) pseudo-Eulerian statistics, in which maps of mean flow kinetic energy (MKE), eddy kinetic energy (EKE), root mean square (r.m.s.) fluctuating velocity magnitude, and mean horizontal flow  $\mathbf{U}(x, y) = (U(x, y), V(x, y))$  are computed from both the model and in situ drifters, considered here as moving current meters; and (b) Lagrangian velocity statistics, in which Lagrangian integral time scales are directly computed from the drifter trajectories.

There are several systematic differences in the nature of the model and observed data that have to be taken into account when performing the comparison. First, the in situ ocean data are from a specific time interval, 1989–1998, while the model-simulated data describe a perpetual year since the model is forced with the same monthly winds and fluxes from 1 year to the next. The in situ drifter data therefore contain inter-annual and high-frequency fluctuations that are absent from the model data. Second, the in situ drifter data are representative of the 15-m deep velocity field, while the model results provide a bulk representation of the variable mixed layer depth, generally between 20 and 100 m, but occasionally reaching 2000 m in winter at high latitudes. For these reasons, complete agreement between the model and the observed data should not be expected. Nevertheless, the comparison can be meaningful in regions where the motion is more related to internal instabilities than to direct atmospheric forcing, as well as in large-scale current structures. The differences between model results and data should provide useful indications for improving further implementations of the model in terms of forcing fields and parameterizations of subgrid scale and mixed layer processes.

The paper is organized as follows: In Section 2, the characteristics of MICOM are discussed. The simulated and in situ drifter data sets are presented in Sections 3 and 4, respectively. The comparison between the data sets is presented in Section 5. A summary and conclusions are provided in Section 6.

## 2. The numerical ocean circulation model

The Miami Isopycnic Coordinate Ocean Model (MICOM) is well documented in the literature. For a

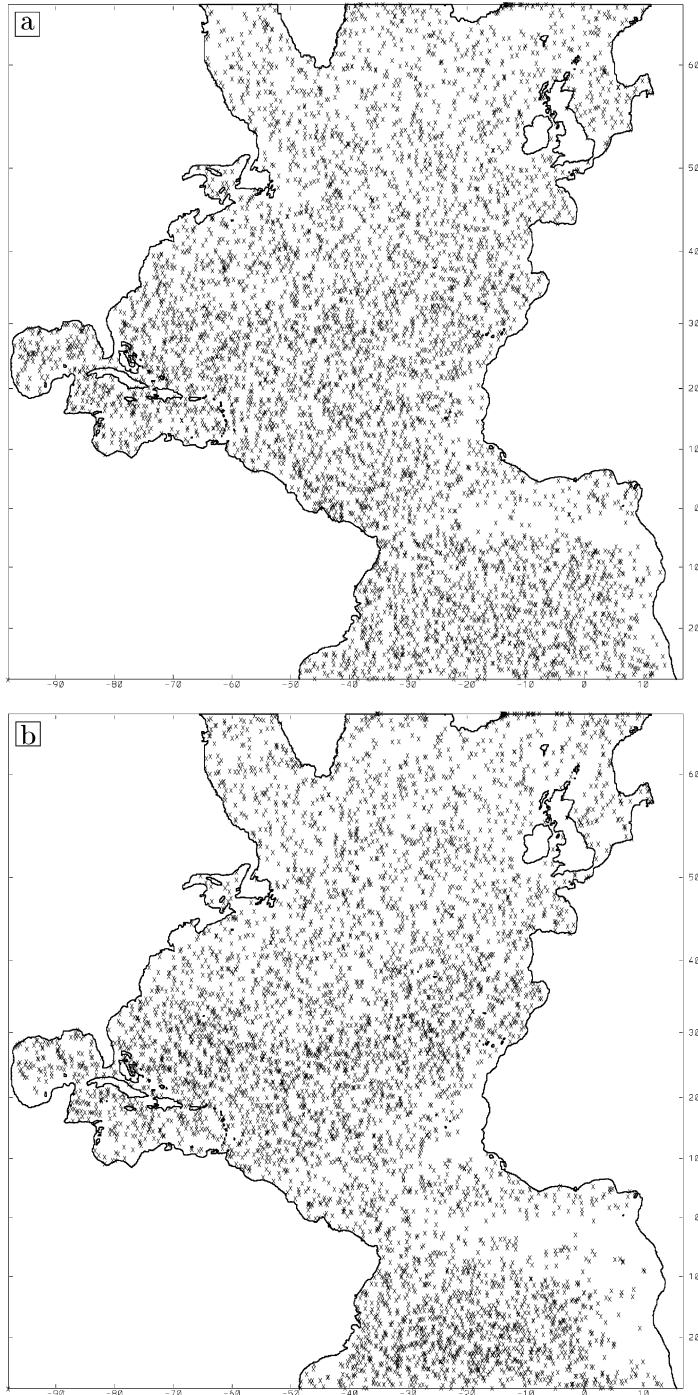


Fig. 1. Location of the model surface numerical Lagrangian floats at (a) the beginning of the analyzed period (August 15, year 14), (b) 300 days later, (c) at the end of the analyzed period (2 years after the initial time). (d) Model float trajectories for a 15-day period beginning on April 6, year 15. (e) Number of model buoy-days/degree<sup>2</sup> for the 2-year period.

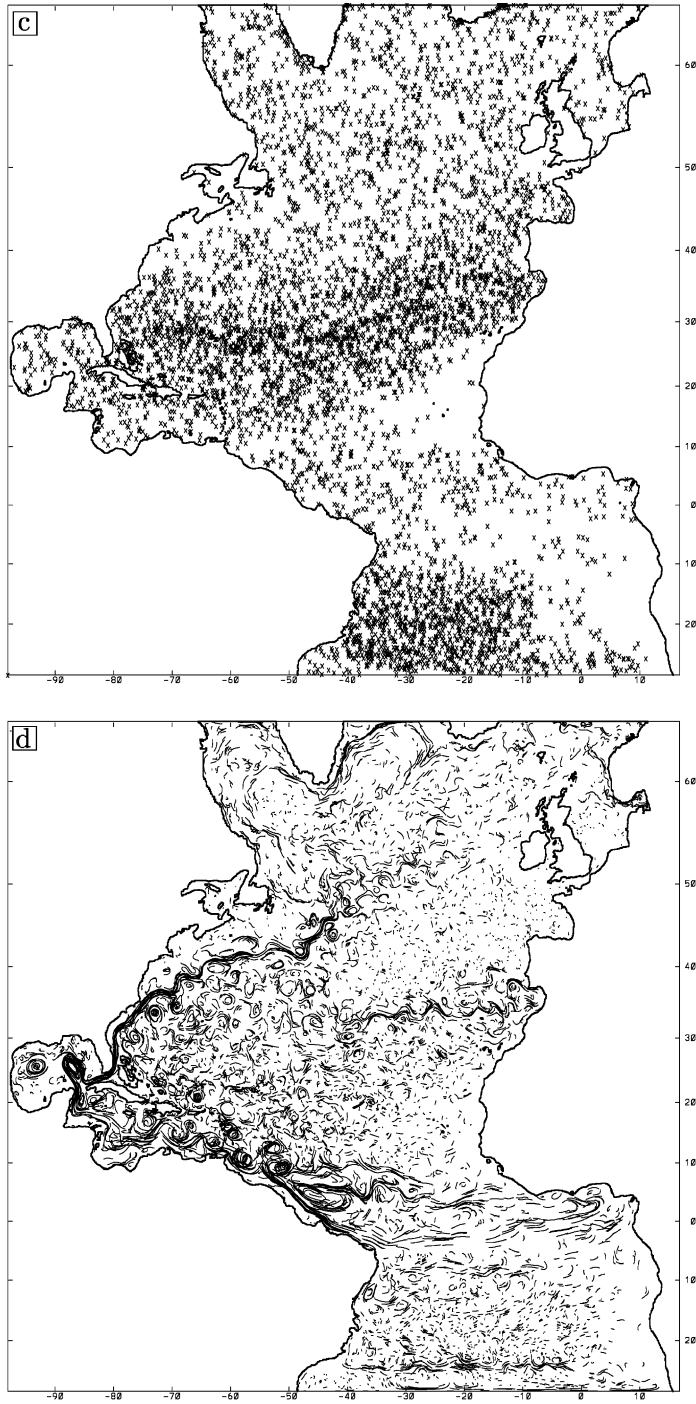


Fig. 1 (continued).

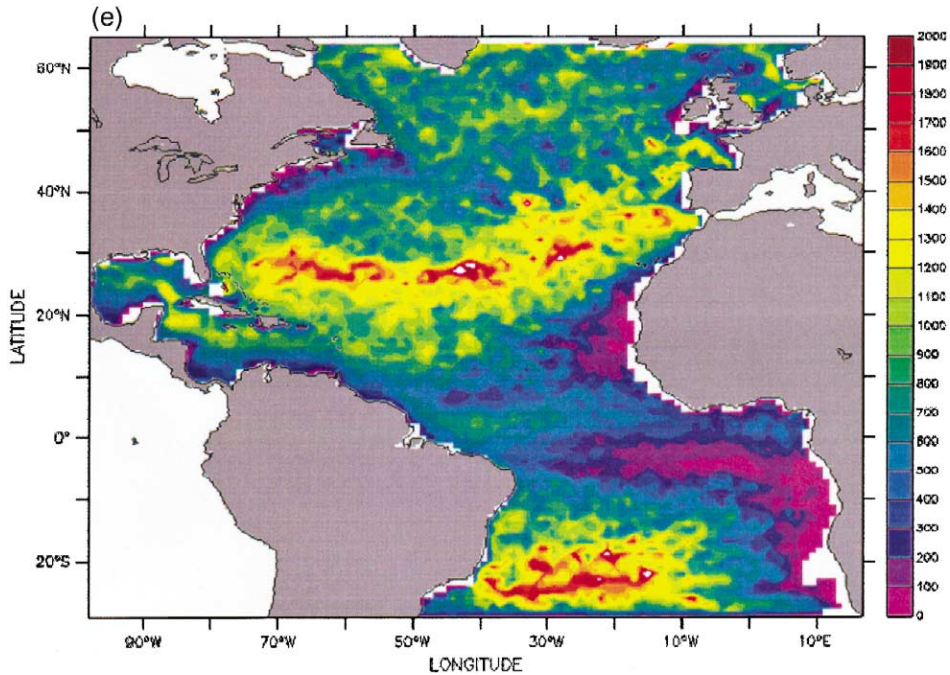


Fig. 1 (continued).

review, the reader is referred to Bleck et al. (1992) and Bleck and Chassignet (1994). The fundamental reason for modeling ocean flow in density coordinates is that this system suppresses the diapycnal component of numerically caused dispersion of material and thermodynamic properties (temperature, salinity, etc.). This characteristic allows isopycnal models to prevent the warming of deep water masses, as has been shown to occur in models framed in Cartesian coordinates (Chassignet et al., 1996). Furthermore, the association of vertical shear with isopycnal packing and tilting in the ocean makes isopycnal models appropriate for studies of strong baroclinic currents such as the Gulf Stream.

The computational domain is the North and Equatorial Atlantic Ocean basin from 28°S to 65°N, including the Caribbean Sea and the Gulf of Mexico. The bottom topography is derived from a digital terrain data set with 5' latitude–longitude resolution (ETOPO5). The surface boundary conditions are based on the COADS monthly climatological data sets (da Silva et al., 1994). Estimation of the model variability under the present climatological forcing will allow us to assess the impact of daily forcing in

a simulation that is presently in progress. Open ocean boundaries are treated as closed, but are outfitted with 3° buffer zones in which temperature  $T$  and salinity  $S$  are linearly relaxed toward their seasonally varying climatological values (Levitus, 1982), with damping/relaxation time from 5 days at the wall to 30 days at the inner edge of the buffer zone. These buffer zones restore the  $T$  and  $S$  fields to climatology in order to approximately recover the vertical shear of the currents through geostrophic adjustment.

The horizontal grid (6 km on average) is defined on a Mercator projection with resolution given by  $1/12^\circ \times 1/12^\circ \cos(\phi)$ , where  $\phi$  is the latitude. The vertical density structure is represented by 15 isopycnal layers, topped by an active surface mixed layer that exchanges mass and properties with the isopycnal layers underneath. The minimum mixed layer thickness is 20 m. The vertical discretization was chosen to provide maximum resolution in the upper part of the ocean. The computational requirements for basin-scale ocean modeling at this resolution are extreme and demand the latest in high performance computation (Bleck et al., 1995). The model was spun up from rest for a total of 20 years.

The high-horizontal grid resolution drastically improved the model's behavior in comparison to that of previous coarse-resolution simulations. The major improvements are (a) a correct Gulf Stream separation and (b) higher eddy activity. These results support the view that an inertial boundary layer, which results from the fine resolution, is an important factor in the separation process (Özgökmen et al., 1997), and that resolution of the first Rossby radius of deformation is necessary for a correct representation of baroclinic instabilities. The simulated Gulf Stream is highly inertial, meanders strongly, and sheds several cyclonic and anti-cyclonic rings. A discussion of the Gulf Stream separation and comparison with two other high-resolution models for the North Atlantic is presented in Chassignet et al. (2001).

An analysis of the turbulent behavior of the model was performed by Paiva et al. (1999) during the spin-up phase for a 3-year period (years 6–8). Sea surface height variability spectra were computed from the model results and were compared to observations and to results of previous models, within the framework of the geostrophic turbulence theory. Length scales representative of the simulated eddy field were found to compare well with observations based on altimeter data. However, the western boundary current intensity during this spin-up period was overestimated by 35% in comparison to observed values, as a consequence of an increase in the model salinity due to the COADS E-P flux boundary condition. This drift was removed after the spin-up by incorporating a weak relaxation to monthly climatological surface salinities from the Levitus climatology, which also had the detrimental effect of significantly decreasing eddy activity over the Gulf Stream extension. Effects of model surface conditions are thoroughly documented in Paiva and Chassignet (2001). The resulting mean transport of 28.5 Sv in the Florida Straits, however, is close to the observed value of 30 Sv, with a seasonal cycle of the same magnitude and phase as seen in the cable data (Larsen, 1992). In the equatorial region, the number of North Brazil current rings and their characteristics agree well with observations. The impact of these rings on the circulation within the Caribbean Sea and on Gulf of Mexico Loop Current eddies is presently being investigated.

### 3. The simulated model drifter data set

At the beginning of year 14, a total of 25,000 numerical particles were launched at the surface in the mixed layer and at depths of 400, 1000, 1500, and 3000 m (5000 particles at each level). The trajectories and diagnostics were computed for a 2-year period, with the particle positions being saved every 12 h and the Eulerian velocity fields every day. The numerical particles were launched in a regular  $1^\circ \times 1^\circ$  grid, initially motivated by a study on ARGOS optimal design (Roemmich et al., 1999).

We focus on the surface particles, which can be directly compared to the 15-m in situ near-surface drifter-derived velocity. As already noted, the modeled surface velocity fields are representative of the depth-averaged mixed layer, which varies seasonally and with latitude. The numerical particle advection scheme is second-order Runge–Kutta, with 16-point space interpolation in the ocean interior and 4-point space near the coasts. The advection inside the first grid box from the coast is accomplished by interpolation, imposing zero velocity at the first point inside land. Consequently, in the first half-grid box from the coast, the Lagrangian particles have a slightly larger along-coast velocity than that, which would be obtained by linear interpolation from the model with no-slip boundary conditions. This choice was made because of its simplicity and because it minimized the loss of particles near the coast on the computational C-grid. Relatively few cases of “beaching” were observed with this boundary condition (less than 3%). Most of the particles that “beached” followed successive corners along the coast, suggesting errors in particle advection due to space interpolation and time extrapolation (particles are advected with a 2-h time step).

Our analysis uses approximately 2 years of simulated particle trajectories. The spatial distribution of model-simulated drifters is shown in Fig. 1a, b, and c, for the initial time of analysis (year 14), 300 days later, and 2 years later, respectively. Clearly, the number of drifters decreases with time in the southern boundary of the subtropical gyre and in the equatorial upwelling region, and increases with time in the subtropical convergence. Since the seasonal cycle is pronounced in the equatorial upwelling region, we can expect that the decrease in the number

of drifters with time would result in a biased time–mean velocity. Fig. 1d shows the trajectories for all of the numerical drifters, during a 15-day period starting in April of year 15. The upwelling regions are poorly sampled due to horizontal divergence of the wind-driven Ekman flow, while the subtropical convergence region is highly sampled. This can also be seen in the total data density distribution (Fig. 1e), obtained by considering the complete data set at all times.

#### 4. The in situ drifter data set

The complete AOML/NOAA drifter data set for the region 98°W–17°E, 33°S–65°N, during the time period 1989–1998, is used for our analysis. The amount of in situ drifter data is 221,336 buoy-days (number of drifters multiplied by number of days, with drifter positions available every 6 h), approximately 1/20 of the size of the simulated drifter data set (~3,600,000 buoy-days). As can be seen in Fig. 2a, the in situ drifter sampling of our analysis domain greatly increases during 1992 and 1993 and levels off to an approximately constant value of 38,000 buoy-days/year after 1996. The lifetime distribution of the drifters (Fig. 2b) illustrates that, while few drifters can be tracked for 1400 days, many can only be tracked for less than 200 days, with an average lifetime of 238 days. The spatial distribution of the initial releases is shown in Fig. 3a. There are several maxima of concentration, close to the Gulf Stream and in the eastern and northern basins, corresponding to the principal experiment sites with multiple deployments.

The space/time distribution of the in situ drifters is sparser and more complex than the distribution of the numerical drifters, resulting in possible statistical biases. For example, the launching regions close to the Gulf Stream area are situated north of the cold wall, so that it can be expected that most of the drifters do not enter the major stream axis. This point will be discussed in more detail in Section 5. Here, we note that, despite these differences, there are some aspects of the resulting distributions of the two data sets that are qualitatively similar.

The distribution of the in situ drifter data after 300 days from release is shown in Fig. 3b. The

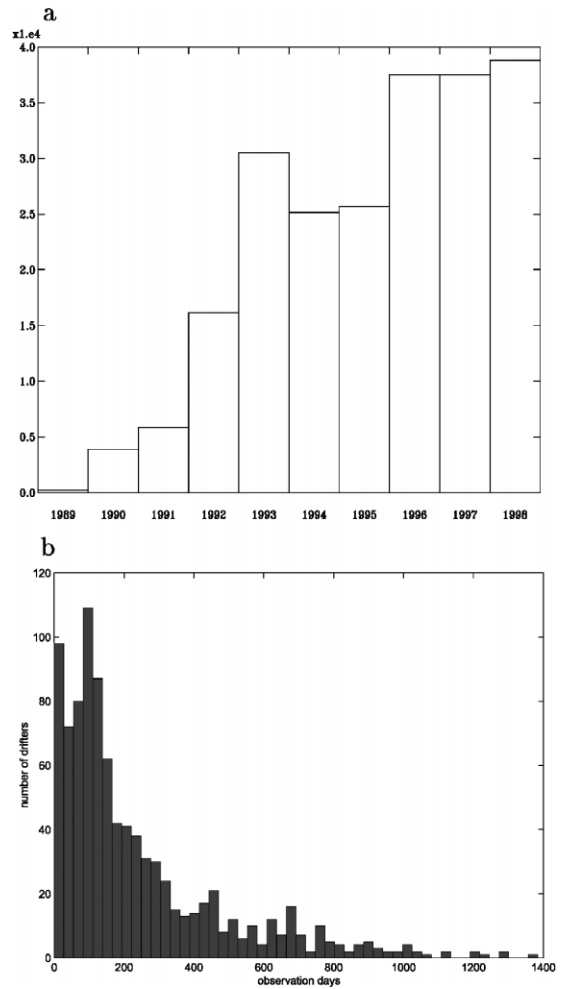


Fig. 2. (a) Number of observations (buoy-days) of the in situ drifters for the period 1989–1998. (b) Life time distribution of the in situ drifters for the same period.

amount of in situ data points has noticeably decreased 300 days after launch, consistently with the lifetime distribution (Fig. 2b). Despite the sparseness of the data, a tendency toward a maximum concentration around 30°N, 25°W is seen, similar to the tendency seen in the model (Fig. 1d,e). It is difficult to determine whether the concentration is due to dynamical convergence as in the numerical data or is a remaining signature of the initial condition concentrations (Fig. 3a). It is worth noticing, however, that no other signatures of initial concentrations are visi-

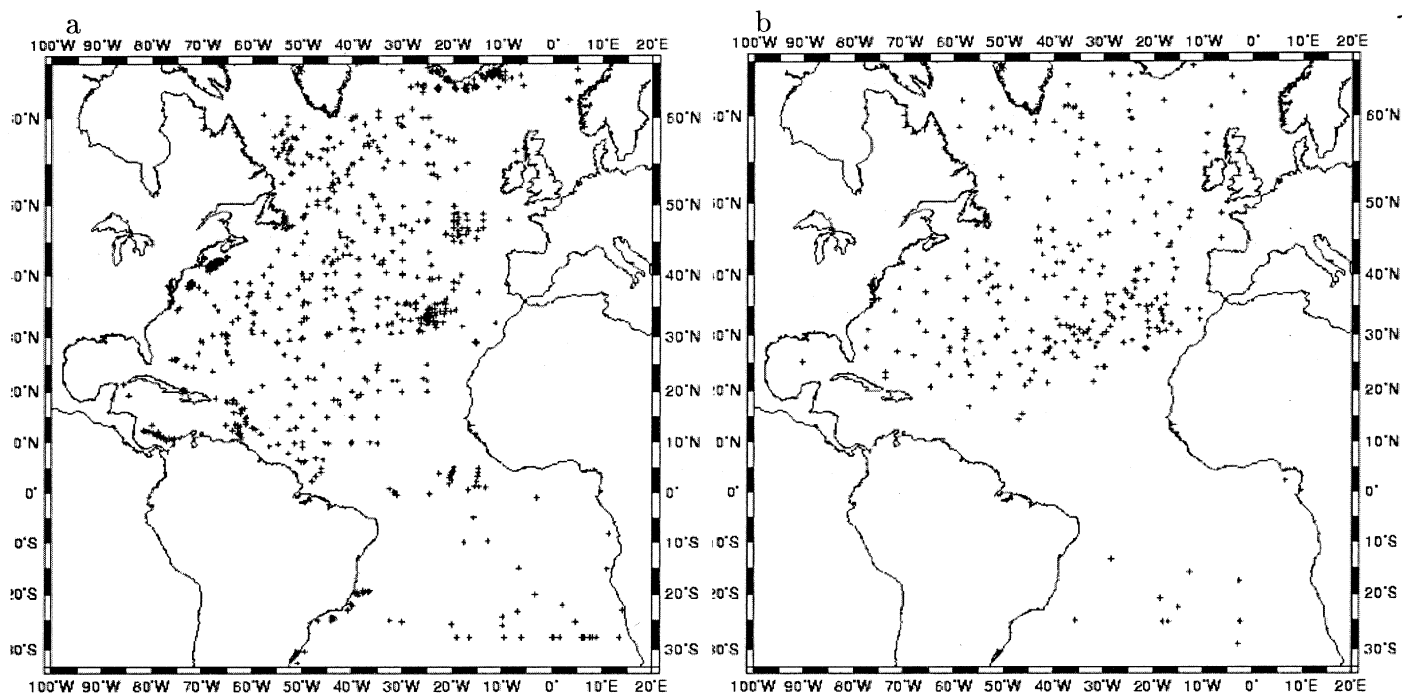
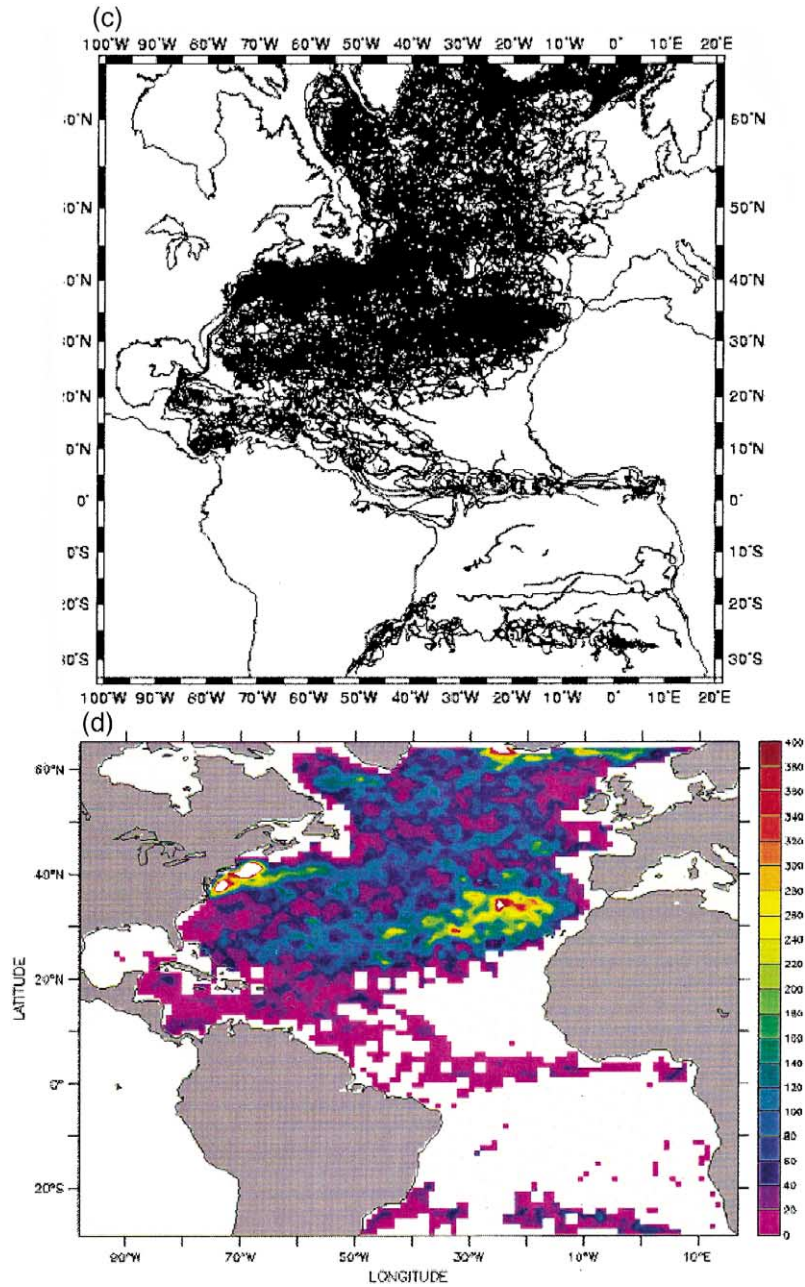


Fig. 3. (a) Launching position of all in situ drifters during the period 1989–1998. (b) Position of the in situ drifters 300 days after launch. (c) Drifter trajectories during their lifetime. (d) Total number of observations for the in situ drifters (buoy-days/degree<sup>2</sup>).



ble in the domain, suggesting the relevance of dynamical convergence.

Also, the “spaghetti” diagram of all in situ trajectories (Fig. 3c) shows a clear absence of data in the

region around 15°N, 25°W, corresponding to the divergence region evident in the model results (Fig. 1b and d). This vacant region in the distribution of in situ drifters is partially due to the lack of initial

releases in the area as well as to the horizontal divergence of the Ekman flow. It is significant that particles do not enter this data-void region from adjacent regions, in agreement with the model results. This tendency is also seen in the maps of total

in situ data density (Fig. 3d), and similarly in the map of the model-simulated drifters (Fig. 1e).

The data density values are smaller for the in situ drifters with maximum values of  $\sim 400$ – $500$  buoy-days per  $1^\circ \times 1^\circ$  box versus  $\sim 2000$  buoy-days for

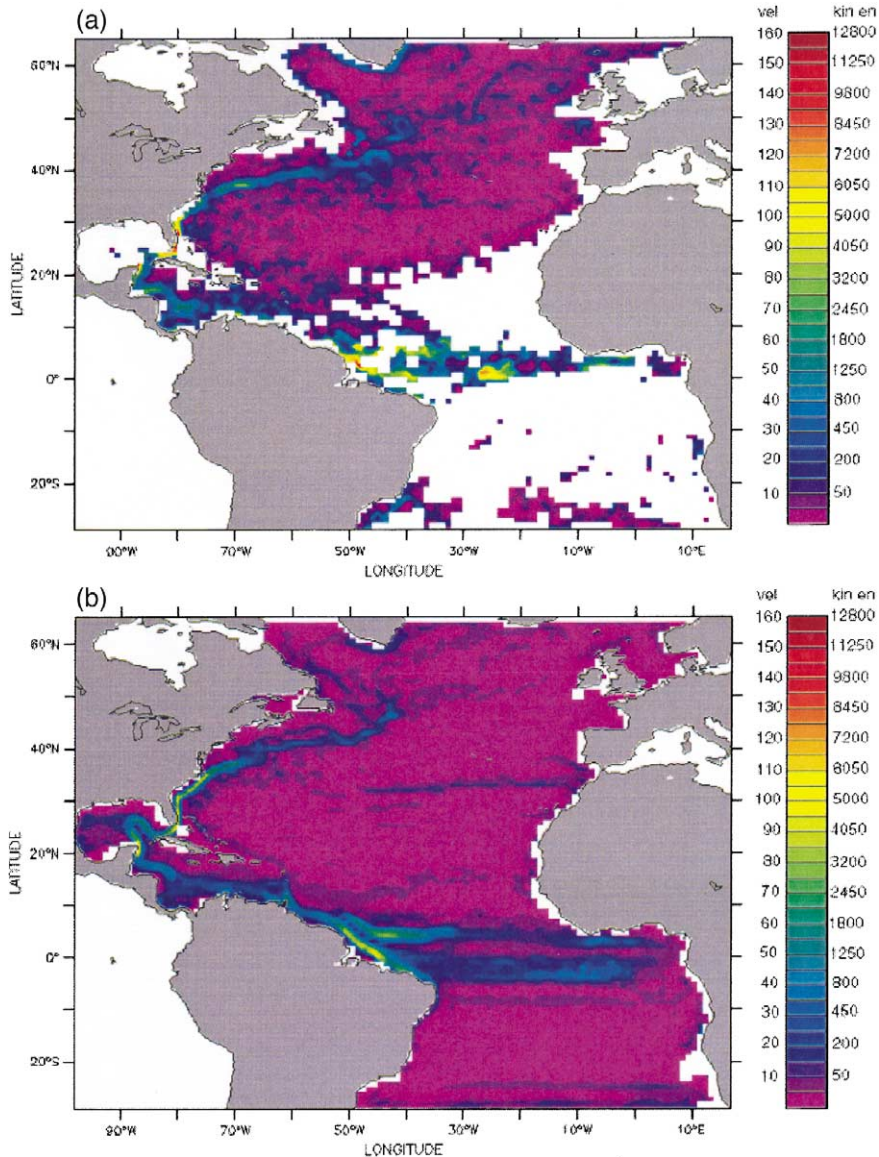


Fig. 4. (a) Mean velocity magnitude  $|\mathbf{U}|$  (cm/s) and mean flow kinetic energy MKE ( $\text{cm}^2/\text{s}^2$ ) for the in situ drifters. (b) Same for the numerical drifters. (c) Difference: model – in situ  $|\mathbf{U}|$  (cm/s). (d) Results of the statistical test: in the blue regions the model and in situ data mean vector velocities  $\mathbf{U}$  differ significantly (at the 95% confidence level); in the yellow regions the difference is not significant; the test is done where the number of independent data is greater than 2.

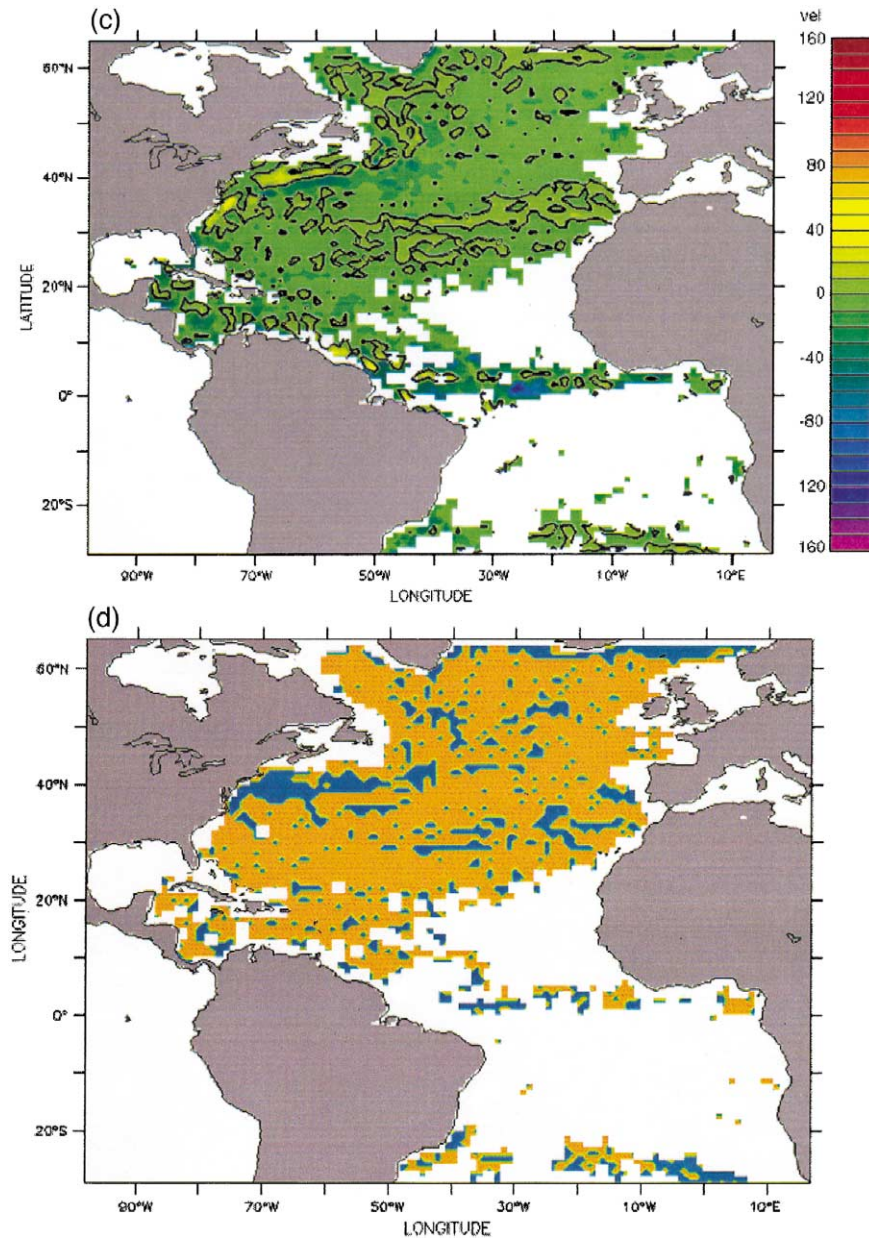


Fig. 4 (continued).

the numerical drifters (in the vicinity of the main experiment releases). Other representative values of data density are  $\sim 150$ – $200$  buoy-days per  $1^\circ \times 1^\circ$  box for the in situ data in the convergence region

versus  $\sim 1500$  for the model drifters, and  $\sim 20$ – $40$  buoy-days per  $1^\circ \times 1^\circ$  box versus  $\sim 800$  for the model drifters in the poorly populated region east of the divergence zone ( $15^\circ\text{N}$ ,  $55^\circ\text{W}$ ).

### 5. Comparison of statistical quantities

In this section, a comparison between model and in situ drifters is performed by considering the following statistical quantities: the mean flow  $\mathbf{U}(x, y)$ , the mean flow kinetic energy (hereafter MKE), the eddy kinetic energy (hereafter EKE), or equivalently mean velocity magnitude and eddy r.m.s. velocity, and the Lagrangian velocity time scale denoted by

$\mathbf{T} = (T_u, T_v)$ . Analysis and results are presented in the following, first discussing the Eulerian quantities and then the Lagrangian.

#### 5.1. Eulerian quantities

The MKE, the EKE, and the mean flow  $\mathbf{U}(x, y)$  are “pseudo-Eulerian” quantities, in the sense that they are Eulerian statistics computed from La-

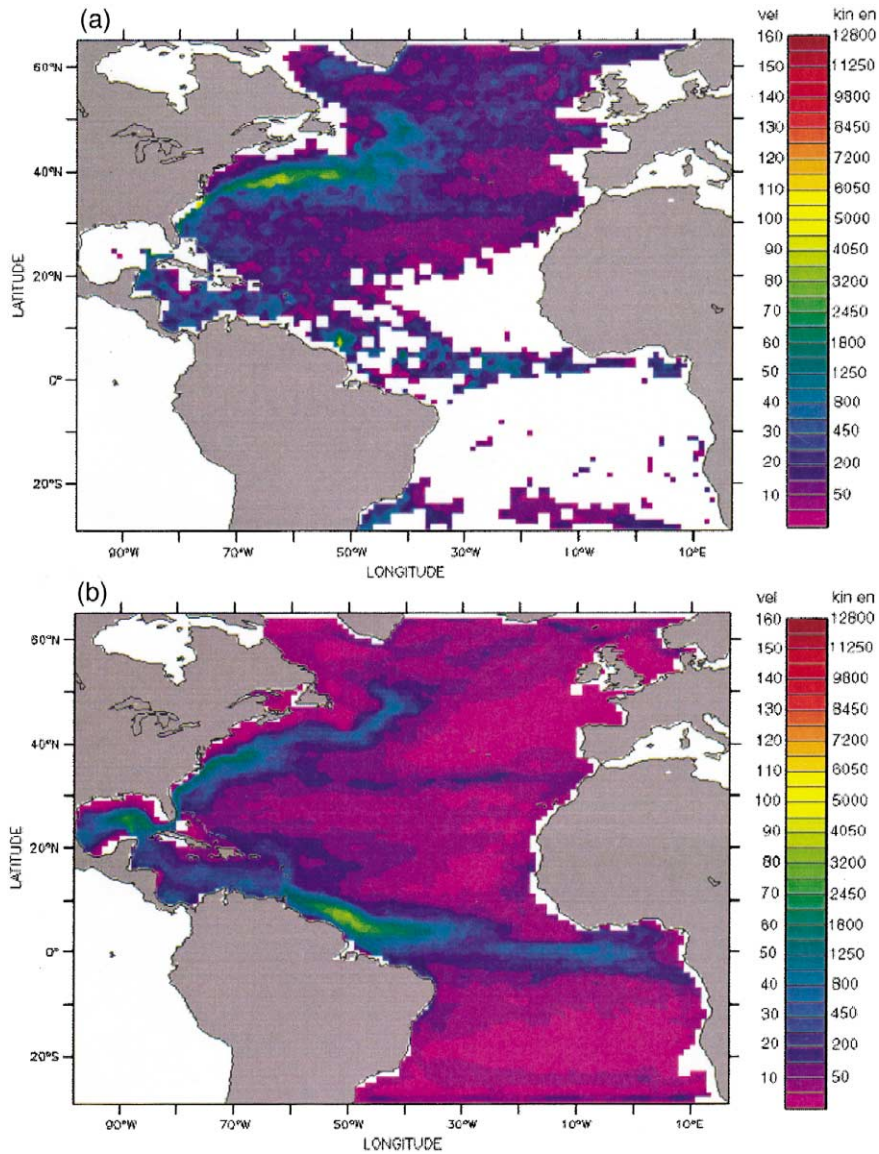


Fig. 5. (a) Eddy velocity magnitude  $u'_{rms}$  (cm/s) and eddy kinetic energy EKE ( $\text{cm}^2/\text{s}^2$ ) for the in situ drifters. (b) Same for the numerical drifters. (c) Difference: model – in situ  $u'_{rms}$  (cm/s).

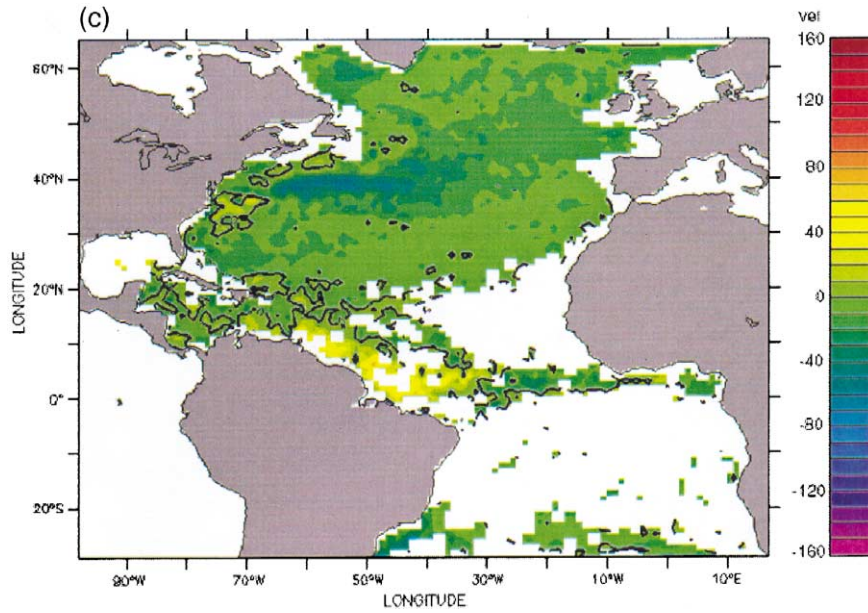


Fig. 5 (continued).

grangian data. Both the model and the in situ drifters are considered for these calculations to be moving current meters, with the velocities  $\mathbf{u}(x, y, t)$  calculated along trajectories by finite differences of the positions. MKE, EKE and  $\mathbf{U}(x, y)$  are estimated using the classical “binning” method (e.g., Owens, 1991), i.e., grouping the velocity data in bins of selected size, here  $1^\circ$  longitude  $\times$   $1^\circ$  latitude. In each bin,  $\mathbf{U}(x, y)$  is computed as the average of all available velocity measurements  $\mathbf{u}(x, y, t)$ , while the fluctuation field,  $\mathbf{u}'$ , is defined as the deviation of  $\mathbf{u}(x, y, t)$  from  $\mathbf{U}(x, y)$ . The MKE is  $1/2(U(x, y)^2 + V(x, y)^2)$  and the EKE  $1/2(\langle u'(x, y)^2 \rangle + \langle v'(x, y)^2 \rangle)$  (see Figs. 4 and 5). Velocities are computed at the midpoint between two successive particle locations. Alternative methods can be used to compute  $\mathbf{U}(x, y)$ , involving for example the use of bi-cubic splines (Bauer et al., 1998) or objective mapping (Davis, 1998), but here we focus on the binning techniques for which the error analysis is more straightforward, allowing for a more direct quantitative comparison. The  $1^\circ$  bin size was chosen because it is about twice the Rossby radius of deformation at the middle of the domain, it is the “average” separation of the simulated drifters, and it

resolves the narrow currents. The bins are taken uniform to keep the analysis simple.

An important point to be addressed before going into the details of the results is the investigation of error sources for estimates of both data sets. Errors include measurement errors for the in situ drifters; model uncertainties primarily dominated by errors in forcing, model physics, numerical discretization, and parameterization of turbulence for the numerical drifters; and errors due to nonstationary and heterogeneous ocean dynamics. Quantifying these errors is not straightforward, and, as a first step, they are neglected in this study.

Another principal source of errors is the data distribution, which leads both to sampling errors related to the number of data available and to the subgrid scale variability, and to bias errors, which are themselves related to gradients of data density, time sampling intervals, and eddy drift (Freeland et al., 1975; Mockett, 1999; Davis, 1991, 1998). Sampling errors and biases for the numerical drifters have been analyzed in detail for mean flow estimates in a companion paper (Garraffo et al., 2001), showing that biases are consistently smaller than sampling errors associated with finite sampling and subgrid

scale processes. For in situ data, a direct estimate of the bias errors cannot be reliably computed; nevertheless, it appears reasonable to assume that even in this case the sampling errors are higher than the biases, given that the data density is lower and the subgrid scale variability is higher for in situ data. As a consequence, sampling errors alone are considered in the quantitative comparison of the mean flow estimates presented in the following.

We notice that, in order to reduce problems coming from the different data distributions in the two data sets, numerical drifters could have been, in principle, sampled in the same way as in situ drifters. We do not expect that this approach would have directly improved the comparison, for two main reasons: (a) model and data differ due to lack of inter-annuality in the model as well as possible differences in current positions, so that there is not necessarily a well-defined correspondence between model/in situ time and space points; and (b) there are relatively few in situ data, so that using the same sampling would significantly increase the sampling error in the numerical data set, making the comparison even less significant. On the other hand, considering a numerical distribution similar to that of the in situ data might be useful in providing an indirect indication of bias errors, and this approach will be considered in future work using ad hoc numerical data.

### 5.1.1. Qualitative comparison

A qualitative comparison of data and model results is first performed by visual inspection of the estimated quantities. MKE and EKE have been computed from both the in situ and numerical drifter data, as well as mean velocity magnitude and eddy r.m.s. velocity,  $|\mathbf{U}| = \sqrt{U^2 + V^2} = \sqrt{2\text{MKE}}$ ;  $u'_{\text{rms}} = \sqrt{\langle u'^2 \rangle + \langle v'^2 \rangle} = \sqrt{2\text{EKE}}$ . Since the values of MKE and EKE cover a vast range in the ocean, comparison of linear maps of MKE and EKE is not an appropriate way to visualize differences in both high-velocity and more quiescent regions. In order to facilitate the visual comparison, we have chosen to map mean and r.m.s. eddy velocity magnitudes (Figs. 4 and 5) instead of kinetic energies, keeping a double scale in the figures, which allows identifying energy values in the various regions.  $|\mathbf{U}|$  ( $u'_{\text{rms}}$ ) maps of

model and in situ data are shown in Fig. 4a,b (Fig. 5a,b), while the difference between model and in situ results is shown in Fig. 4c (Fig. 5c).

The comparison between the  $|\mathbf{U}|$  of the model and in situ drifters appears to be overall satisfactory (Fig. 4), even though the  $|\mathbf{U}|$  map for the in situ data is relatively noisy due to the lower data density.  $|\mathbf{U}|$  values in the Gulf Stream are similar for model and observations, even though the model values are slightly lower: model values are of  $\approx 80$  cm/s ( $\text{MKE} \approx 3200 \text{ cm}^2/\text{s}^2$ ) west of 65W, and  $\approx 30$  cm/s ( $\text{MKE} \approx 450 \text{ cm}^2/\text{s}^2$ ) in the extension east of 65W; in situ values show isolated maxima higher than 100 cm/s ( $\text{MKE} 5000 \text{ cm}^2/\text{s}^2$ ) in the Florida Current, and are  $\approx 40$  cm/s east of 65W ( $\text{MKE} \approx 800 \text{ cm}^2/\text{s}^2$ ). Interior values are also similar, of the order of 5 cm/s. At a more detailed level, some differences can be noted. The Gulf Stream extension path appears to be located approximately 200 km farther north in the model than in the observations (Fig. 4c). The Azores Current has a more extended signature in the model (with  $|\mathbf{U}| \approx 10\text{--}15$  cm/s,  $\text{MKE} \approx 50\text{--}110 \text{ cm}^2/\text{s}^2$ ), while the North Equatorial and North Brazil currents seem to be underestimated in the model, showing maximum  $|\mathbf{U}|$  values of  $\approx 80\text{--}100$  cm/s ( $\text{MKE} \approx 3200\text{--}5000 \text{ cm}^2/\text{s}^2$ ) versus observational maximum values of  $\approx 100$  cm/s ( $\text{MKE} \approx 5000 \text{ cm}^2/\text{s}^2$ ). The issue of significance of these differences, as function of data density and variability, will be quantified in the following using James test.

Regarding the pattern of eddy variability,  $u'_{\text{rms}}$  maps (Fig. 5) of model and observations show more marked differences than those of the mean flow. Maximum  $u'_{\text{rms}}$  values are associated with the main currents. In the Gulf Stream, they reach values of  $\approx 65$  cm/s ( $\text{EKE} \approx 2100 \text{ cm}^2/\text{s}^2$ ) in the model and  $\approx 80\text{--}100$  cm/s ( $\text{EKE} \approx 3200\text{--}5000 \text{ cm}^2/\text{s}^2$ ) in the observations. Also, the high-energy region influenced by the extension is bigger in the observation than in the model. This suggests that, even though the mechanisms of baroclinic and barotropic instabilities are reproduced by the model, the extent of the variability is underestimated.

In the North Equatorial and Brazil currents, the model shows high values of variability,  $u'_{\text{rms}} \approx 80$  cm/s ( $\text{EKE} \approx 3200 \text{ cm}^2/\text{s}^2$ ), apparently overestimating the in situ values. As already mentioned with

respect to the mean flow, though, the sparseness of the data in this area does not allow to draw a firm conclusion. It is interesting to notice that the total kinetic energy (MKE + EKE, not shown) is closely comparable for model ( $\approx 6000 \text{ cm}^2/\text{s}^2$ ) and in situ data ( $\approx 6000\text{--}7000 \text{ cm}^2/\text{s}^2$ ).

In the interior ocean away from the major currents and in the northern part of the domain,  $u'_{\text{rms}}$  is higher in the in situ data, with values that reach  $\approx 15\text{--}25 \text{ cm/s}$  (EKE  $\approx 110\text{--}310 \text{ cm}^2/\text{s}^2$ ), whereas in the model they reach  $\approx 10\text{--}15 \text{ cm/s}$  (EKE  $\approx 50\text{--}110 \text{ cm}^2/\text{s}^2$ ). This is presumably due to the lack of high-frequency winds in the model forcing, leading to underestimation of the directly forced eddy variability. This effect is amplified in the northern regions during late winter, when the momentum of already too weak winds is distributed through very deep mixed layers. The fact that some of the in situ data are tracked only every 3 days can lead to an overestimation of EKE, thus possibly accounting for some of the differences.

### 5.1.2. Quantitative comparison

A more quantitative comparison is now presented for the vector velocity,  $\mathbf{U}(x, y)$ , for which the nature of the statistical error as a first-order statistical quantity is well understood. Since the model variability is smaller than that of the observations, we use James' statistical test for comparing two vectors with different variances [following the notation of Seber (1984, pp. 114–117)]. In the remainder of this section, the two independent sets of vector samples from our population space consist of near-surface mean horizontal ocean velocities, namely, the spatially dependent average of the in situ data velocity and of the model Lagrangian velocity, denoted by  $\mathbf{U}_d$  and  $\mathbf{U}_m$ , respectively.

We test to see if the differences  $\mathbf{U}_m - \mathbf{U}_d$  are significant, given the uncertainties in each set of estimates of the mean flow. Our null hypothesis is that  $\mathbf{U}_m$  and  $\mathbf{U}_d$  are equal:

$$H_0: \mathbf{U}_m - \mathbf{U}_d = 0,$$

and a test statistic for the null hypothesis is:

$$(\mathbf{U}_m - \mathbf{U}_d)^\dagger \left( \frac{1}{n_m} \mathbf{S}_m + \frac{1}{n_d} \mathbf{S}_d \right)^{-1} (\mathbf{U}_m - \mathbf{U}_d) \quad (1)$$

where  $\dagger$  indicates a matrix transpose.  $\mathbf{S}_m$  and  $\mathbf{S}_d$  are the covariance matrices of the model and in situ drifter velocities.  $n_m$  and  $n_d$  are the corresponding number of independent data points. The number of independent data is calculated (e.g., Owens, 1991) as the number of data points in the bin (Figs. 1e and 3d) divided by twice the corresponding integral time scale (the computation of  $\mathbf{T}$  is discussed in Section 5.2 and the values are shown in Fig. 6). For the cross-covariance between the two velocity components, the time scale is taken as the average of the two time scales from each direction. Notice that, strictly speaking, the spatial correlation of the measurements should also be considered, introducing an appropriate space scale; however, this aspect is not considered here. For the initial horizontal seeding resolution of  $1^\circ$ , which is approximately twice the baroclinic Rossby radius of deformation at mid-latitudes, the approximation is well motivated given that particle trajectories are fairly uncorrelated. The upper  $\alpha$  critical value,  $k_\alpha$ , correct to order  $n^{-2}$ , is

$$k_\alpha = \chi_2^2(\alpha) [A + B\chi_2^2(\alpha)],$$

where

$$A = 1 + \frac{1}{4} \sum_{i=1}^2 \frac{1}{n_i - 1} \left( \text{tr} \left[ \frac{\mathbf{S}_T^{-1} \mathbf{S}_i}{n_i} \right] \right)^2,$$

$$B = \frac{1}{8} \left[ \sum_{i=1}^2 \frac{1}{n_i - 1} \left( \frac{1}{2} \left( \text{tr} \left[ \frac{\mathbf{S}_T^{-1} \mathbf{S}_i}{n_i} \right] \right)^2 + \text{tr} \left[ \frac{\mathbf{S}_T^{-1} \mathbf{S}_i}{n_i} \right]^2 \right) \right],$$

$$\mathbf{S}_T = \frac{1}{n_m} \mathbf{S}_m + \frac{1}{n_d} \mathbf{S}_d,$$

where  $i = 1, 2$  correspond to the model and in situ data, respectively.

The modified  $\chi^2$  value is found to be approximately 6.5 for an  $\alpha$  value of 0.05. When the test statistic (Eq. (1)) is greater than the modified  $\chi^2$  value, the model and data are said to differ significantly. We would reject the null hypothesis of equal means for those regions with a possibility of being incorrect 5% of the time. The areas in which the

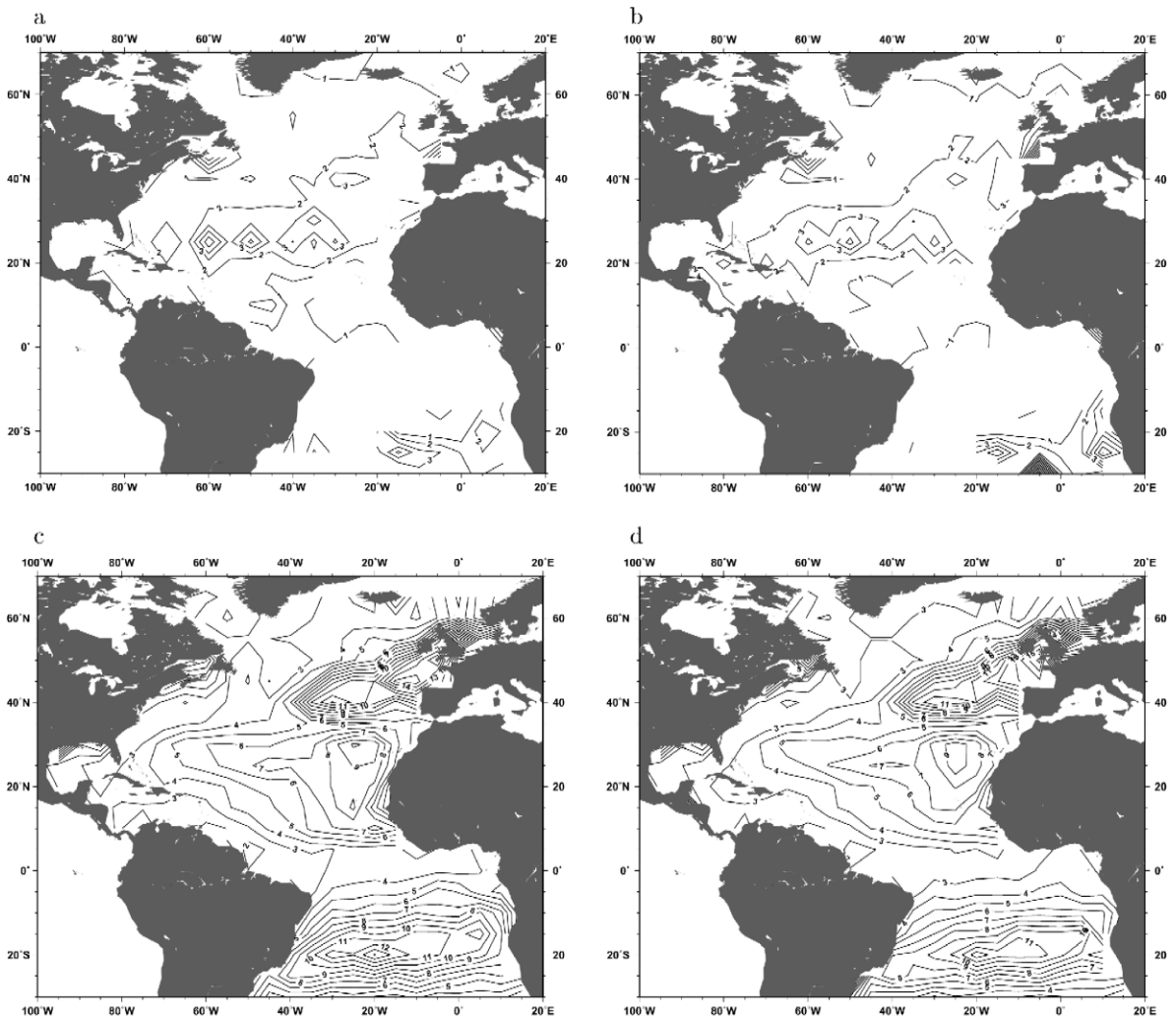


Fig. 6. Lagrangian velocity integral time scale in days for the (a) zonal and (b) meridional directions, for all in situ drifters in the region. (c,d) Same for the model drifters.

model and in situ data are significantly different are indicated by the blue regions in the plot shown in Fig. 4d. It is clear that the simulated and observed in situ near-surface velocities are not significantly different over most of the domain.

The regions of disagreement between model and in situ data are primarily the Gulf Stream after the separation point and the Azores Current. It is important to reemphasize here the fact that these results are strongly dependent on the data density. The differences in the Azores Current and in the Gulf Stream are significant because of the large number

of in situ measurements (Fig. 3). On the other hand, more measurements are needed in the North Equatorial region to assess the model's performance.

Large-velocity differences in the Gulf Stream region can occur when there is a relatively small error in the path of that current. These results indicate that, on average, the model Gulf Stream remains approximately 200 km too far north in comparison to its observed position. This seems to be a fairly robust conclusion, in view also of the following two facts. First, as mentioned in Section 4, in situ drifters were primarily deployed north of the wall. This might

cause biases in the estimates of Gulf Stream position and energetics, but very unlikely can induce a southern bias for the position. Also, an independent test of this model/data difference is provided by satellite observations of the mean Gulf Stream extension location, which is located less than 200 km south respect to the model location (Chassignet et al., 2001).

Buffer zones—including the zone for the Gulf of Cadiz, which drives the Azores Current in the model (Özgökmen et al., 2001)—are also problematic given that, in these areas, climatological statistics in the model, which lack forcing at inter-annual and high-frequency periods and are constrained by restoring to climatological oceanic data, are being compared to statistics from in situ observations of oceanic motion that contain a broad continuum of scales. Therefore, it is not surprising that significant differences appear close to the buffer zones, primarily in the Azores Current and in the far northern regions of the model domain.

## 5.2. Lagrangian quantities

The other principal statistical quantity that is considered is the Lagrangian velocity time scale  $\mathbf{T} = (T_u, T_v)$ , a purely Lagrangian quantity defined for the two velocity components as:

$$T_u = \frac{1}{\sigma_u^2} \int_0^\infty R_{uu}(\tau) d\tau,$$

and

$$T_v = \frac{1}{\sigma_v^2} \int_0^\infty R_{vv}(\tau) d\tau.$$

$\mathbf{R}$  is the Lagrangian temporal auto-covariance function, computed for  $u$  and  $v$  following particles, and defined as:

$$R_{uu}(\tau) = \langle (u(t) - \bar{u}(t))(u(t + \tau) - \bar{u}(t)) \rangle,$$

$$R_{vv}(\tau) = \langle (v(t) - \bar{v}(t))(v(t + \tau) - \bar{v}(t)) \rangle,$$

where the symbol  $\langle \rangle$  indicates expected values.

The estimates of  $\mathbf{T}$  (shown in Fig. 6) are calculated by first dividing the drifter trajectories into segments whose first and last positions are 400 km apart. Four hundred kilometers is chosen as a compromise in order to have sufficient data to reliably

calculate temporal covariance functions and also to resolve the spatial details of the eddy field. All “leftover” segments or short trajectories containing at least 50 positions are also used in the analysis. For each velocity component,  $\mathbf{R}$  is estimated computing the expected value,  $\langle \rangle$ , as an arithmetic average over all data with lag  $\tau$ . The average velocities,  $\bar{u}(t)$ ,  $\bar{v}(t)$ , are given by a least-squares fit to a linear trend using 400 km long subsets of a drifter’s trajectory. The variances of  $u$  and  $v$ , denoted by  $\sigma_u^2$  and  $\sigma_v^2$ , are  $\mathbf{R}_{uu}(0)$  and  $\mathbf{R}_{vv}(0)$ , respectively.

When  $\mathbf{R}$  is calculated from a finite data set, a subjective choice for the limits of integration to compute  $\mathbf{T}$  must be made. To avoid this problem and to gain statistical confidence, a function of a small number of parameters is fitted to each temporal auto-covariance function  $\mathbf{R}$ ,

$$\mathbf{R}(\tau) = \sigma^2 (1 - \epsilon_n^2) \cos(2\pi\tau/P) e^{-(\tau/\tau_e)^2},$$

where  $\epsilon_n^2$  is the normalized (by total variance  $\sigma^2$ ) variance of subgrid scale processes and measurement variance for the data,  $P$  is the period that equals four times the zero-crossing scale of the covariance function, and  $\tau_e$  is the e-folding scale or the turbulent time scale. This covariance function, based on a smoothed version of a second-order auto-regressive process, contains a wave component and a turbulent component, and produces excellent fits to the observed and simulated Lagrangian velocity covariance functions.

The three parameters ( $\epsilon_n^2$ ,  $P$ , and  $\tau_e$ ) are determined using the feature-based technique described in Mariano and Chin (1996), which finds the value of  $R(\tau)$  at zero lag ( $= \sigma^2(1 - \epsilon_n^2)$ ), finds the zero-crossing scale of  $\mathbf{R}$  ( $= P/4$ ) by determining where  $\mathbf{R}(\tau)$  changes from positive to negative, and finds the e-folding scale  $\tau_e$  from the first two parameters, an initial guess consisting of the lag at which  $\mathbf{R}(\tau)$  is  $1/e$  of its initial value, and the best fit being determined in a least-squares sense.

The time scales, computed for each 400 km long subset of a drifter trajectory, are determined by evaluating the integral of  $\mathbf{R}(\tau)$  (Gradshteyn and Ryzhik, 1980, p. 477),

$$\int_0^\infty \mathbf{R}(\tau) d\tau = \sigma^2 (1 - \epsilon_n^2) \frac{\tau_e}{2} \sqrt{\pi} \exp\left(\frac{-\pi^2 \tau_e^2}{P^2}\right),$$

using the estimated three parameters and  $\sigma^2$ . Then, the integral time scale is

$$\mathbf{T} = (1 - \epsilon_n^2) \frac{\tau_e}{2} \sqrt{\pi} \exp\left(\frac{-\pi^2 \tau_e^2}{P^2}\right).$$

Direct numerical integration of the temporal auto-covariance functions, using  $n$  temporal lags, requires estimating  $n$  parameters for the integration. Each of these  $n$  parameters is noisy and small changes in  $n$  can cause large changes in the value of the integral. This is especially true when the temporal auto-covariance function has large negative lobes. The integration of the Lagrangian velocity auto-covariance function using three parameters leads to more robust estimates of the Lagrangian velocity time scales than does the numerical integration of  $n$  values of  $\mathbf{R}(\tau)$ .

The values of  $\mathbf{T}$  are assigned to the midpoint of the drifter trajectory. A least-squares bi-cubic smoothing spline (Inoue, 1986) is then used to interpolate the estimates of  $\mathbf{T}$  to a regular grid. The plots shown in Fig. 6 are contoured to a  $5^\circ \times 5^\circ$  grid to enhance the large-scale structure of the Lagrangian velocity time scales.

### 5.2.1. Qualitative comparison

In the following, a qualitative comparison of estimates of  $\mathbf{T}$  for numerical and in situ data is presented. Error estimates of Lagrangian quantities such as  $\mathbf{T}$  were not performed. Lagrangian velocity integral time scales  $\mathbf{T}$  calculated for both the model and in situ drifters are isotropic over most of the basin (Fig. 6). An exception to this is the anisotropy noted in the tropical Atlantic in the model results, where  $T_u$  is longer than  $T_v$ . However, an insufficient amount of in situ data in that region makes it impossible to confirm this model result. The basic pattern of model results shows that time scales are longer in the eastern Atlantic, especially in the northern region off Europe. Isolines extend tongue-like from the eastern boundaries, and the lowest values are found close to the major currents of the western boundaries. Results from in situ data are of course much sparser, since a reduced number of bins have sufficient data to support the time scale computation. The resulting pattern is sketchy, nevertheless, there is an indication of a tongue-like shape of the isolines extending from the eastern boundaries resembling the numerical re-

sults. There is also a hint of high  $\mathbf{T}$  values in the northeast region, close to the coast of the UK.

Regarding the values of the time scales, the model appears to overestimate these by a factor of two, most likely due to the use of climatological monthly winds in the model simulation and to the loss of the effects of variability in the wind forcing as a result of the model's slab mixed layer formulation. Also, the integral time scales of the in situ drifters may underestimate the true near-surface Lagrangian velocity time scales because the drifters are not perfect Lagrangian devices; they can "slip" in the water, resulting in a velocity error on the order of 2 cm/s.

## 6. Summary and concluding remarks

In this paper, a comparison has been presented between the statistics of in situ and simulated drifter trajectories in the North Atlantic. The space and time distribution of the two data sets are different. Model drifters were homogeneously seeded in a regular  $1^\circ$  grid, having a constant lifetime of approximately 2 years. The in situ drifters, on the other hand, have inhomogeneous initial conditions, and lifetimes with an average of 238 days and maximum values of approximately 1400 days. Despite these differences, the total data distributions computed over the complete data sets show some similarities. Both distributions, in fact, appear to be influenced by the large-scale convergence patterns related to Ekman flow. This is especially apparent in the model results, since the drifter lifetime is sufficiently long to allow a clear representation of the phenomenon, but it is also detectable in the in situ data, in the subtropical convergence region and in the southeastern divergence region.

The distribution and properties of the eddy field were compared using two types of statistics, the pseudo-Eulerian EKE and  $u'_{\text{rms}}$  and the Lagrangian time scale  $\mathbf{T}$ . The model  $u'_{\text{rms}}$  reproduces the location for the maxima and minima of the in situ data, but quantitatively the model  $u'_{\text{rms}}$  values show a number of differences from the in situ values. In the Gulf Stream,  $u'_{\text{rms}}$  is greater in the in situ data and it extends over a larger area than that calculated from the model results. In the North Equatorial and Brazil

currents, the model seems to overestimate  $u'_{rms}$ , even though the results are not robust due to the sparseness of in situ data. In the interior, the model underestimates the eddy energy, very likely because of the lack of high-frequency winds in the model forcing, leading to an underestimation of directly forced eddies. This effect is amplified in the winter northern regions, when the momentum is distributed over a deep mixed layer. The lack of a vigorous eddy field in the interior is suggested also by the comparison of the time scales  $T$ , which are longer in the model than in the observations by approximately a factor of 2, indicating overly smooth trajectories. It should also be mentioned that since the numerical trajectories were computed directly from a velocity field produced by the model (smoothed by the dissipation operator), they are excessively smooth. The subgrid scale actions could be “re-introduced” in the trajectories using, for instance, a stochastic model (e.g., Dutkiewicz et al., 1993), which would help to reduce  $T$ . Tests along these lines are planned for the future.

Regarding the mean flow structure, a quantitative comparison has been performed using James’ statistical test. The statistical errors considered in this test, for both simulated and in situ data, are the sampling errors related to the number of data available and to the subgrid scale variability. Other error sources, such as measurement errors for the in situ data and model uncertainties in forcing and parameterizations, have been neglected. The results show that the in situ- and model-derived mean flows can be considered different, at a 95% confidence level, primarily in the zone of the Gulf Stream extension and in the Azores Current. Differences in the Gulf Stream region are primarily related to a relatively small error in the path of the current. Even though the model correctly represents the strength of the Gulf Stream, its path still lies somewhat too far north. Differences in the mean Azores Current, as well as differences in the northernmost regions, are likely to be related to the presence of buffer zones representing, respectively, the interaction with the Mediterranean Sea and the Arctic Ocean.

In summary, the comparison has shown that model and in situ estimates of Lagrangian mean flow do not differ significantly over most of the domain, while the eddy field appears to be underestimated by the model in part of the Gulf Stream and in the interior.

The greatest value of such a comparison is that it indicates the weakest point of the model and helps to set directions for improvement. The present results point to the following principal areas for future work: non-climatological high-frequency wind forcing to improve variability in the interior, a non-slab mixed layer formulation for better representation of the surface fields, improved boundary conditions, and subgrid scale parameterization in the trajectory calculation. Concurrently, the in situ drifter database will grow, especially in the tropical Atlantic, to allow more meaningful comparisons.

### Acknowledgements

The authors wish to thank E. Ryan for help in the technical development, E. Zambianchi for several useful discussions, L. Smith for her careful editing of the manuscript, and three anonymous reviewers for their comments. The authors acknowledge the PIs who collected the North Atlantic drifter data and generously made them available through NOAA-AOML. This research was supported by the National Science Foundation through Grant OCE-9811358 and by the Office of Naval Research through Grants ONR N00014-95-1-0257, N00014-97-1-0620, and N00014-99-1-0049. Computations were performed on the Department of Defense (DoD) computers at the Stennis Space Center under a challenge grant from the DoD High Performance Computer Modernization Office.

### References

- Acero-Schertzer, C.E., Hansen, D.V., Swenson, M.S., 1997. Evaluation and diagnosis of surface currents in the National Centers for Environmental Prediction’s ocean analyses. *J. Geophys. Res.* 102, 21037–21048.
- Bauer, S., Swenson, M., Griffa, A., Mariano, A.J., Owens, K., 1998. Eddy-mean flow decomposition and eddy-diffusivity estimates in the tropical Pacific Ocean. *J. Geophys. Res.* 103, 30855–30871.
- Bleck, R., Chassignet, E., 1994. Simulating the oceanic circulation with isopycnic-coordinate models. In: Majundar, S.K. (Ed.), *The Oceans: Physical–Chemical Dynamics and Human Impact*. The Pennsylvania Academy of Science, pp. 17–39.
- Bleck, R., Rooth, C., Hu, D., Smith, L.T., 1992. Salinity-driven thermocline transients in a wind- and thermohaline-forced

- isopycnic coordinate model of the North Atlantic. *J. Phys. Oceanogr.* 22, 1486–1505.
- Bleck, R., Dean, S., O'Keefe, M., Sawdey, A., Numrich, R.W., 1995. A comparison of data-parallel and message-passing versions of the Miami Isopycnic Coordinate Ocean Model (MICOM). *Parallel Comput.* 21, 1695–1720.
- Chassignet, E.P., Smith, L.T., Bleck, R., Bryan, F.O., 1996. A model comparison: numerical simulations of the North and Equatorial Atlantic oceanic circulation in depth and isopycnic coordinates. *J. Phys. Oceanogr.* 26, 1849–1867.
- Chassignet, E.P., Garraffo, Z.D., Smith, R.D., Hurlburt, H.E., 2001. High resolution Gulf Stream modeling. *Ocean Modelling*, submitted.
- da Silva, A.M., Young, C.C., Levitus, S., 1994. Atlas of surface marine data. Technical Report. National Oceanic and Atmospheric Administration.
- Davis, R.E., 1991. Observing the general circulation with floats. *Deep-Sea Res.* 38, 531–571.
- Davis, R.E., 1996. Comparison of autonomous Lagrangian circulation explorer and fine resolution Antarctic model results in the South Atlantic. *J. Geophys. Res.* 101, 855–884.
- Davis, R.E., 1998. Preliminary results from directly measuring middepth circulation in the tropical and South Pacific. *J. Geophys. Res.* 103, 24619–24639.
- Dutkiewicz, S., Griffa, A., Olson, D., 1993. Particle diffusion in a meandering jet. *J. Geophys. Res.* 98, 16487–16500.
- Freeland, H.J., Rhines, P., Rossby, H.T., 1975. Statistical observations of trajectories of neutrally buoyant floats in the North Atlantic. *J. Mar. Res.* 33, 383–404.
- Garraffo, Z.D., Griffa, A., Mariano, A.J., Chassignet, E.P., 2001. Lagrangian data in a high resolution numerical simulation of the North Atlantic. II. On the pseudo-Eulerian averaging of Lagrangian data. *J. Mar. Syst.* 29, 177–200.
- Gradshteyn, I.S., Ryzhik, I.M., 1980. In: Jeffrey, A. (Ed.), *Table of Integrals, Series, and Products*. Academic Press, New York, Translation by Scripta Technica, 1160 pp.
- Inoue, H., 1986. A least-square smooth fitting for irregularly spaced data: finite-element approach using the cubic B-spline basis. *Geophysics* 51, 2051–2066.
- Larsen, J.C., 1992. Transport and heat flux of the Florida Current at 27°N derived from cross-stream voltages and profiling data: theory and observations. *Philos. Trans. R. Soc. London* 338, 169–236.
- Levitus, S., 1982. *Climatological Atlas of the World Ocean*. NOAA Professional Paper 13, US Dept. of Commerce, NOAA.
- Mariano, A.J., Chin, T.M., 1996. Feature and contour based data analysis and assimilation in physical oceanography. In: Adler, Muller, A., Rozovskii, J. (Eds.), *Stochastic Modeling in Physical Oceanography*. Birkhauser, Boston, MA, pp. 311–342.
- Mockett, C., 1999. Dispersion and reconstruction. Summer GFD Program, WHOI technical report 99–01, pp. 166–188.
- Özgökmen, T.M., Chassignet, E.P., Paiva, A., 1997. Impact of wind forcing, bottom topography, and inertia on mid-latitude jet separation in a quasi-geostrophic model. *J. Phys. Oceanogr.* 27, 2460–2476.
- Özgökmen, T.M., Chassignet, E.P., Rooth, C.G., 2001. On the connection between the Mediterranean outflow and the Azores Current. *J. Phys. Oceanogr.* 28, 257–303.
- Owens, W.B., 1991. A statistical description of the mean circulation and eddy variability in the northwestern North Atlantic using SOFAR floats. *Prog. Oceanogr.* 28, 257–303.
- Paiva, A.M., Chassignet, E.P., 2001. The impact of surface flux parameterizations on the modeling of the North Atlantic Ocean. *J. Phys. Oceanogr.*, in press.
- Paiva, A.M., Hargrove, J.T., Chassignet, E.P., Bleck, R., 1999. Turbulent behavior of a fine mesh (1/12 deg) numerical simulation of the North Atlantic. *J. Mar. Syst.* 21, 307–320.
- Roemmich, D., Boebel, O., Desaubies, Y., Freeland, H., King, B., Le Traon, P.-Y., Molinari, R., Owens, W.B., Riser, S., Send, U., Takeuchi, K., Wijffels, W., 1999. ARGO: the global array of profiling floats. *Ocean Obs 99 Conference*, San Raphael, France.
- Seber, G.A.F., 1984. *Multivariate Observations*. Wiley, New York, 686 pp.
- Stutzer, S., Krauss, W., 1998. Mean circulation and transport in the South Atlantic Ocean: combining model and drifter data. *J. Geophys. Res.* 103, 30985–31002.